universität wien

MASTERARBEIT / MASTER'S THESIS

Titel der Masterarbeit / Title of the Master's Thesis

„Improving the mobility of nanoscale zero-valent iron in granular matrix by means of aquifer modification"

verfasst von / submitted by

Florian Marko, BSc

angestrebter akademischer Grad / in partial fulfilment of the requirements for the degree of

Master of Science (MSc)

Wien, 2015 / Vienna 2015

Studienkennzahl lt. Studienblatt / degree programme code as it appears on the student record sheet:	A 066 815
Studienrichtung lt. Studienblatt / degree programme as it appears on the student record sheet:	Masterstudium Erdwissenschaften
Betreut von / Supervisor:	Univ. Prof. Dr. Thilo Hofmann
Mitbetreut von / Co-Supervisor:	

Abstract

In situ remediation of groundwater with nanoscale zero-valent iron (nZVI) particles is governed by *inter alia* particle mobility, which is greatly influenced by surface heterogeneities of mineral grains. Previous studies demonstrated enhanced particle stabilization and mobility in granular matrices when negatively charged polyelectrolytes were applied as suspension-additive. Negatively charged polyelectrolytes are hereby proposed to be used as "aquifer modifiers" under assumption that they can screen positively and weakly negatively charged surfaces of the mineral grains and with it promote mobility of nZVI. This thesis addresses the influence of pre-injected lignin sulfonate and humate (hereafter aquifer modifiers) solutions on mobility of polyacrylic acid-coated nZVI (PAA-nZVI) in well-controlled columns filled with granular matrix. Solutions of aquifer modifiers showed different effects on nZVI mobility, depending on their concentration and the type of water they are prepared in. Without pre-injection of aquifer modifiers, nZVI suspension prepared in divalent cation-rich standardized EPA water was practically immobile, while nZVI suspension prepared in ultrapure water reached a breakthrough of ca. 0.32. Pre-injection of aquifer modifiers in in ultrapure water had no effect on nZVI mobility. Nevertheless, the application of humate in EPA water increased the nZVI breakthrough significantly, resulting in a theoretical maximal transport distance of 37 cm when conducted with 100 mg L^{-1}. Finally, humate appeared to have higher potential to enhance nZVI mobility for longer period of time.

Zusammenfassung

Die experimentellen Ergebnisse dieser Studie zeigen, dass die Pre-Injektion von negativ geladenen Polyelektrolyten (Ligninsulfonat und Humat, hiernach Aquifermodifizierer) in natürlichen Quarzsand die Mobilität von nZVI Partikeln unter gut kontrollierten Laborbedingungen steigern kann.

In ultrareinem Wasser konnte das zeta (ζ) potential von Quarzsand mit Ligninsulfonat und Humat dauerhaft gesenkt werden. In EPA Wasser, welches eine hohe Ionenstärke besitzt, blieb des ζ Potential des Quarzsandes konstant. Der Anteil an divalenten Kationen im EPA Wasser schwächte zusätzlich das ζ Potential der nZVI Partikel und reduzierte die elektrostatische sowie elektrosterische Abstoßung zwischen den Partikeln. Folglich vergrößerte sich der durchschnittliche Aggregatsdurchmesser und die nZVI-Partikel wurden immobil in EPA Wasser, während der nZVI Durchbruch in ultrareinem Wasser 0.32 erreichte.

Pre-injektion von Aquifermodifizierern zeigte keinen Effekt auf den nZVI-Transport in ultrareinem Wasser. Jedoch konnte der nZVI Durchbruch in EPA Wasser gesteigert steigern, wenn Humat in einer Konzertration von 100 mg L^{-1} pre-injiziert wurde. Die theoretische maximale Transportdistanz der Partikel $L_{T\ 0.001}$ wurde hierbei auf 37 cm verlängert. Zusätzlich durchgeführte Langzeit-Transportexperimente könnten darauf hinweisen, dass Humat unter Bedingungen in der Natur auch bei länger andauernden nZVI-Injektionen der wirksamere Aquifermodifizierer ist.

Die Transportkoeffizienten, berechnet nach der *Colloid Filtration Theory*, zeigten einen Anstieg der theoretischen maximalen Transportdistanz $L_{T\ 0.001}$ bei Reduzierung von *attachment efficiency* und *first order removal rate*. Es ist zu bemerken, dass die benutzten Sandkörner und nZVI keine uniforme Größe sowie perfekte Kugelform besitzen, wie in der *Colloid Filtration Theory* angenommen. Des Weiteren muss beachtet werden, dass alle Experimente unter gut kontrollierten Laborbedingungen durchgeführt wurden.

Um einen möglichst vollständigen Einblick über die Effekte und Wirkungsweisen der zwei getesteten Aquifermodifizierer zu bekommen, sind weitere detaillierte Analysen derer Moleküle und zusätzliche Transportexperimente mit niedrigeren und höheren Konzentrationen notwendig.

Die Experimente lieferten Hinweise dafür, dass die kleinste und mobilste Fraktion der nZVI Partikel während des Experimentdurchlaufes oxidiert worden sein könnte, was deren Reaktivität mit Schadstoffen möglicherweise mindern würde. Bevor eine entsprechende Feldanwendung durchgeführt werden sollte, bedarf es weiterer Erforschung dieses möglichen Effektes.

Im Hinblick auf eine effektive Verteilung der nZVI-Partikel im kontaminierten Untergrund ist eine weitere Verbesserung des nZVI-Transportes unabdingbar. Verglichen zu EPA Wasser kann kontaminiertes Grundwasser beträchtlich größere Anteile an multivalenten Kationen und eine höhere Ionenstärke aufweisen. Weiters beinhaltet Aquifermaterial einen höheren Anteil an chemischen und physikalischen Heterogenitäten, welche den nZVI-Transport zusätzlich beinträchtigen können.

List of Figures and Tables

Fig. 1 Tentative monomeric structures of lignin sulfonate and humic acid..... 5

Fig. 2 Experimental setup for column experiments 8

Fig. 3 SEM image of NANOFER S25 particles 12

Fig. 4 ζ potential of quartz sand as a function of lignin sulfonate and humate concentration in MQ and EPA background solution 14

Fig. 5 Aquifer modifier breakthrough C/C_0 in MQ and EPA water during injection into the column and during flushing the column with background solution after aquifer modifier injection 16

Fig. 6 Total iron breakthrough as a function of concentration of pre-injected lignin sulfonate and humate in MQ and EPA water..... 18

Fig. 7 Total iron breakthrough of long term transport experiments as a function of concentration of pre-injected lignin sulfonate and humate in MQ and EPA water 20

Fig. 8 Increase of theoretical transport length $L_{T\,0.001}$ of nZVI as a function of first order removal rate k_{CFT} and the attachment efficiency α in MQ and EPA water 22

Fig. 9A Sieving curve of Dorsilit Nr.8 as a function of Φ Values according to Tucker et al. (2001).....37

Fig. 10A Sampled suspension of white particle fraction flushed out oft the column.....38

Tab. 1 Ionic composition, electronic conductivity (EC) and pH of EPA moderately hard water 6

Tab. 2 Chemical composition and sedimentological properties of the sand.....12

Tab. 3A Recorded parameter during ζ potential measurements and long-term measurements of the sand in different aquifer modifier solutions..... 37

Tab. 4A Transport coefficients for nZVI calculated following Colloid Filtration Theory (Section 2.8).....39

Tab. 5A Fitted MNMs model parameters for nZVI transport.....39

Tab. 6A Fitted MNMs model parameters for aquifer modifier transport.....40

Table of Contents

Abstract i

Zusammenfassung ii

List of Figures and Tables iv

1 Introduction 1

2 Material and Methods 3

2.1 Nanoscale zero-valent iron particle suspension 3

2.2 Granular matrix 4

2.3 Aquifer modifiers 4

2.4 Background solutions 5

2.5 Zeta potential of the sand 6

2.6 Column experiments 7

2.7 Calculation of transport parameters following the colloid filtration theory (Elimelech et al., 1995; Kretzschmar et al., 1999; Tufenkji & Elimelech, 2004) 8

2.8 Transport model 9

2.8.1 Modeling transport of nZVI 9

2.8.2 Modeling transport of aquifer modifiers 10

3 Results and Discussion 11

3.1 Characterization of nZVI suspension 11

3.2 Characterization of sand 12

3.3 Surface charge of natural sand and effect of aquifer modifiers 13

3.4 Interaction between aquifer modifiers and natural sand 14

3.5 Effect of pre-injected aquifer modifiers on nZVI transport 17

3.6 Long-term effect of pre-injected aquifer modifiers on nZVI transport 19

3.7 Calculated parameters and model coefficients of nZVI transport 21

4 Conclusions and implications for field injection 23

5 Acknowledgements 25

6 References 25

6.1 Internet links 36

7 Appendix 37

7.1 Appendix 1 – Properties of the natural sand 37

7.2 Appendix 2 – Calculated transport coefficients and MNMs model output data 39

7.3 Statutory Declaration 41

7.4 Curriculum Vitae 42

1 Introduction

In situ remediation of groundwater with nanoscale zero-valent iron (nZVI) particles is being an intensively studied technique. Due to its high specific surface area and reactivity nZVI can be applied to treat chlorinated organics, pharmaceuticals, heavy metals and radionuclides (Zhang, 2003; Grieger et al., 2010; Kanel et al., 2005; Li & Zhang, 2007; Stieber et al., 2008).

Because of its high reactivity and a broad spectrum of treatable pollutants the nZVI-based remediation technology is proposed to lower the overall remediation time and be a cost-effective alternative to frequently applied remediation techniques, such as pump-and-treat and can be directly injected in the subsurface of the field site (Tratnyek & Johnson, 2006; Karn et al., 2009; Chang & Kang, 2009). In contrast to conventional permeable reactive barriers, nZVI injection can directly treat multiple contaminated sources, contamination situated in deeper aquifers and in subsurface beneath aboveground infrastructure.

nZVI used in groundwater remediation is applied in form of a suspension, which is injected into the subsurface. Therefore, nZVI mobility must be sufficient to accurately transport and distribute the particles into the contaminated zones within the aquifer (Crane & Scott, 2012). Mobility of nZVI in the subsurface is greatly affected by the injection technique, the injection velocity, and particle concentration (Phenrat et al., 2010; Raychoudhury et al., 2010; Laumann et al., 2013), which all can be controlled during the injection. Nevertheless processes of aggregation, sedimentation, pore blocking and attachment onto the aquifer grains still limit the mobility of nZVI in aquifers (Laumann et al., 2014; Johnson et al., 1996; Hofmann & Von der Kammer, 2009). The impact of these processes to nZVI mobility depends on the particle properties (e.g., particle size, size distribution, surface charge) as well as physical and chemical heterogeneities encountered in aquifers such as surface charge heterogeneities, grain size distribution, porosity, varying mineralogy and content of natural organic matter (NOM) (Phenrat et al., 2009; Johnson et al., 1996; Laumann et al., 2013).

nZVI particles are composed of a Fe^0 core surrounded by a thin iron oxide shell (Crane et al., 2011). Polyelectrolytes are polymers with ionizable groups, which

dissociate in water and have a strong tendency to adsorb to solid surfaces (Dobrynin & Rubinstein, 2005; Borcovec & Papastavrou, 2008). By coating nZVI particles with such anionic polyelectrolytes with high molecular weight, the positive surface charge resulting from the iron oxide shell is reversed to negative. Therefore, particle coating enhances electrostatic and steric repulsion thus decreasing agglomeration and deposition onto negatively charged surfaces in porous media (Kim et al., 2012; Phenrat et al., 2009).

However, mineralogical diversity and chemical impurities in the aquifer (e.g., iron oxides, NOM, carbonate and clay minerals; Ryan & Elimelech, 1996; Phenrat et al., 2009; Laumann et al., 2013) provide positively charged or weekly negatively charged surfaces at the mineral grains that limit the mobility of nZVI. Previous research proofed that these positively as well as weakly negatively charged patches on mineral surfaces function as favorable deposition sites for negatively charged nZVI particles (Johnson et al., 1996; Laumann et al., 2013; Chen et al., 2011). In addition, natural groundwater often contains divalent cations like Ca^{2+} and Mg^{2+}, which cause aggregation of nanoparticles via charge neutralization, compression of the electronic double layer, bridging, and other mechanisms, hence additionally reducing the mobility of nZVI in the aquifer (Saleh et al., 2008; Dong & Lo, 2013a; Chen et al., 2007a).

One approach towards suppressing the attachment of nZVI onto the mineral surfaces and towards enhancement of transport of nZVI in heterogeneous porous aquifers is to increase the electrostatic and steric repulsions between nZVI and mineral surfaces. Modifying the aquifers by means of pre-injection of anionic polyelectrolytes (hereafter “aquifer modifiers”) prior to the injection of nZVI into subsurface is an approach proposed to “screen” surface heterogeneities within the aquifer and finally promote the mobility of nanoparticles used in groundwater remediation.

Several studies used polyelectrolytes as additive to suspensions of non-coated nZVI particles and assessed their influence on nZVI transport in porous media (Jones & Su, 2012; Johnson et al., 2009; Jiemvarangkul et al., 2010; Phenrat et al., 2009). Furthermore, Laumann et al. (2014) showed that lignin sulfonate co-injected with nZVI doubles the transport distance of polyacrylic acid (PAA)-coated nZVI in artificial and freshly crushed carbonate sand.

The objective of this thesis is to evaluate the applicability of two proposed aquifer modifiers in enhancing the transport of nZVI. Accordingly, following subjects have been addressed: (a) the effect of pre-injection of aquifer modifiers (lignin sulfonate and humate; prepared in different background solutions and at different concentrations) onto mobility of commercial available nZVI in granular matrices (b) the effect of pre-injection of these modifiers on the surface charge of granular matrices (c) the "long term" effect of pre-injected modifiers on transport of nZVI, and (d) prediction of transport parameters of nZVI in granular matrices before and after aquifer modification following the colloid filtration theory and applying MNMs software tool .

2 Material and Methods

2.1 Nanoscale zero-valent iron particle suspension

The nZVI (NANOFER 25S, NANO IRON s.r.o., Czech Republic) are coated with polyacrylic acid (PAA) and preserved in an aqueous stock suspension. Referring to the producer, this stock suspension has an pH of 11–12, a mean primary particle diameter <50 nm and Fe_{tot} concentration of ~ 20 wt.% with a specific surface area of 25 $m^2\ g^{-1}$ (http://www.nanoiron.cz/en/nanofer-25s). Previous research investigated transport and stability of NANOFER 25S (Dong & Lo, 2013; Laumann et al., 2013 and 2014; Lerner et al., 2012), as well as its reactivity (Schmid et al., 2015; Li et al., 2012) and ecotoxicology (Kadar et al., 2011; Keller et al., 2012).

The nZVI suspensions for the column experiments carried out in this study were diluted from the stock suspension either with ultrapure water (Millipore, Elix®5-Milli-Q® Gradient A10; thereafter MQ) or EPA water (see Section 2.4) to a Fe_{tot} concentration of ~ 1 g L^{-1} and sonicated for 15 min (ultrasonic bath, Sonorex RK 106, Bandelin electronic, Germany) before injected into the columns in order to prevent aggregation of particles.

The particle size distribution and average sizes were determined in the 1 g L^{-1} Fe_{tot} suspensions using laser diffraction method (MASTERSIZER 2000, Malvern Instruments, UK).

Electrophoretic mobility of the particles was analyzed in the diluted suspensions (prepared in MQ and EPA water) using laser Doppler velocimetry (Zetasizer Nano ZS, Malvern Instruments, UK). The conversion of electrophoretic mobility to the zeta

potential was calculated via the Smoluchowski relationship (Hunter, 1988).

The Fe_{tot} concentration was determined using inductively coupled plasma optical emission spectroscopy (ICP-OES, Optima 5300DV, PerkinElmer, USA) after digestion with hydrochloric and nitric acid.

2.2 Granular matrix

The granular matrix used was Dorsilit sand (Dorsilit® Nr. 8 Kristallquarz, Gebrüder Dorfner GmbH & Co., Germany), mainly consisting of quartz.

The grain size distribution of this sand was determined by wet sieving. Fractions of 0.063–0.125, 0.125–0.25, 0.25–0.5, 0.5–1, 1–2, 2–4 and >4 mm were collected, oven-dried and weighed.

In order to determine the bulk chemistry of the sand, samples were grinded and investigated with ICP-OES (Optima 5300DV, PerkinElmer, USA) after acid digestion. The total organic carbon (TOC) content was inspected with LECO RC612 Carbon Analyzer (LECO Corporation, USA).

The effective porosity of the sand was determined using a nonreactive NaBr tracer test injected into the columns prior to each experiment (Section 2.6).

2.3 Aquifer modifiers

Two different polyelectrolytes were applied as aquifer modifiers: humate (Humin-S775, Humintech GmbH, Germany; thereafter HU), containing 70–80% humic acids according to the producer and lignin sulfonate (N18, Otto Dille GmbH, Germany; thereafter LS). The randomly branched polyelectrolytes are complex in terms of chemical structure, size and composition and possess multiple functional groups. Both producers did not provide details on the molecular structure of these polyelectrolytes. Fig. 1 highlights schematically the typical functional groups of lignin sulfonate (e.g. sulfonic, carboxylic and phenolic hydroxyl groups) and humic acid (e.g. carboxylic, phenolic and carbonylic groups). Literature reports the molecular weight distribution of LS molecules between <1000 and >100000 Da (Moacanin et al., 1955), molecular weight of humic acid molecules is ranging from 500 to >200000 Da (Stevenson, 1982; Beckett et al., 1987).

The production of both modifiers is inexpensive, which is a precondition for their application in a cost effective remediation. Humic acid is generated by biodegradation of dead organic matter and has been reported to stabilize particles (Le Bell, 1984; Chowdhury et al., 2012) as well as improving their transport (Kretzschmar et al., 1997; Yang et al., 2010). Several studies indicated that humic acid can act as natural surfactant and utilized to remove pollutants from contaminated soils (Wandruszka 2000; Conte et al., 2005; Rebhun et al., 1996).

Lignin sulfonate arises as secondary product of wood pulp manufacture during sulfonication of the bio-macromolecule lignin. Milczarek et al. (2013) showed that lignin sulfonate stabilizes nanoscale silver particles. In addition, Laumann et al. (2014) showed an enhancement in transport of PAA-nZVI with co-injection of lignin sulfonate.

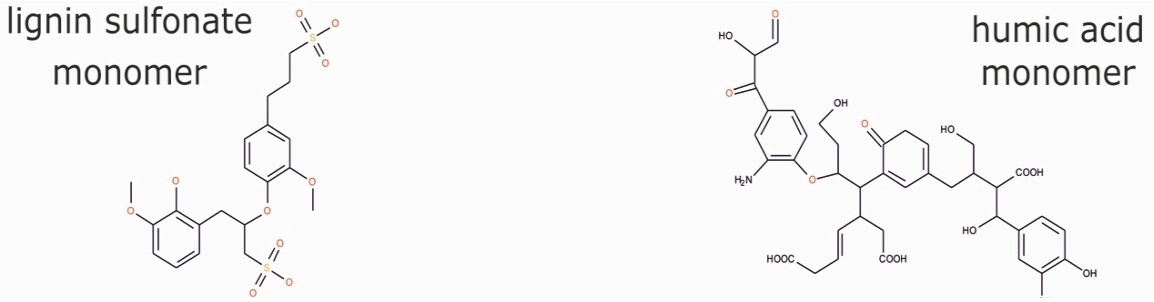

Fig. 1 — Tentative monomeric structures of lignin sulfonate (source: http://www.chemicalregister.com) and humic acid (source: Wandruszka, 2000) adapted by Vesna Micić Batka

2.4 Background solutions

Two types of background solutions have been used: (i) ultrapure MQ water (Elix®5-Milli-Q® Gradient A10, EMD Millipore, USA) with a TOC content <30 ppb, <10 CFU per mL and an electrical resistivity of 10−15 MΩ cm.

In order to account for the effect of divalent ions and ionic strength encountered in natural environment on the nZVI transport (ii) standardized EPA moderately hard water (hereafter EPA water) was applied as additional background solution. The EPA water was prepared as described in US EPA Report EPA-821-R-02-012, Section 7.2.3.1 (US EPA, 2002). The ionic composition and properties of EPA water are shown in Table 1.

Table 1 – Ionic composition, electronic conductivity (EC) and pH of EPA moderately hard water.									
	Na^+	K^+	Ca^{2+}	Mg^{2+}	Cl^-	SO^{2-}	NO^-	EC at 22.6°C [mS m^{-1}]	pH at 25°C
[mg L^{-1}]	26.8	2.3	13.8	11.2	2.2	79.3	0.6	29.7	7.8

2.5 Zeta potential of the sand

The Zeta (ζ) potential of the sand was acquired with an Electrokinetic Analyzer (SurPass, Anton Paar GmbH, Austria) and recalculated from streaming potential following the Fairbrother-Mastin approach (Fairbrother & Mastin, 1924).

8 g of sand were wet-packed into a cylindrical glass cell. A minimum amount of dissolved ions as free mobile charges are a prerequisite for measuring the streaming potential (Verliefde et al., 2009; Juhl et al., 2014; Laumann et al., 2013), therefore the aquifer modifier solutions were prepared in 1 mM NaCl (instead of MQ water) or EPA water. Additionally to the intrinsic parameter detection in SurPass, electric conductivity and pH of the background solutions were (WTW LF318 and WTW 340i, WTW Wissenschaftlich-Technische Werkstätten GmbH, Germany).

The determination of ζ potential was carried out as 3-step procedure:

(1) Measuring the initial ζ potential of the sand in pure background solution (1 mM NaCl or EPA water).

(2) Exchanging the background solution with the aquifer modifier solution and measuring the changes in the ζ potential after the equilibration time of around 15 min (according to Laumann et al., 2014).

(3) In order to simulate a long-term effect of modifiers on the sand's surface the modifiers solution was newly exchanged with a fresh background solution (1 mM NaCl or EPA water) and the ζ potential was recorded again after ~ 15 min of equilibration time.

2.6 Column experiments

Transport experiments have been performed following the procedure of Schmid et al. (2015):

Column experiments were carried out in borosilicate glass columns (∅ 2.5 cm, 15 cm length; Omnifit, Germany). Each column was wet packed with the sand to a height of 10 cm and flushed with at least ten pore volumes (PVs) of background solution (MQ or EPA water) in order to remove background turbidity. A peristaltic pump (Ismatec, Germany) was used to pump the background solutions, solutions of tracer and aquifer modifiers, and nZVI suspensions into the columns with an effective injection velocity of ~ 100 m d^{-1}. The injections were conducted from bottom to keep the columns constantly saturated and facilitate degassing (Lewis & Sjöstrom, 2010).

The effective porosity of the sand was determined by means of a conservative NaBr (30 mg L^{-1}) tracer. The Br^- concentration in the effluent was quantified by ion chromatography (ICS-1000, Dionex, Austria). All transport experiments were run at minimum in duplicates. Furthermore, two pressure gauges were mounted to one of the columns (one at the inlet and the outlet, as seen in Fig. 1) and the pressure changes were continuously recorded.

The tracer solution was then flushed with a background solution (MQ or EPA water), prior to introduction of the solution of aquifer modifiers (~ 10 PVs) in concentrations of 50 or 100 mg L^{-1}. The concentration of aquifer modifier in the effluent was analyzed using UV-Vis spectroscopy (LAMBDA 35, PerkinElmer, USA) at wavelengths of 280 nm and 254 nm for lignin sulfonate (Lekelefac et al., 2014; Laumann et al., 2014) and humate respectively (Weishaar et al., 2003). The limits of detection (LOD) and limits of quantification (LOQ) for UV-Vis spectroscopy were calculated after Wankhede et al. (2012) and resulted in 0.5 mg L^{-1} (LOD) and 1.5 mg L^{-1} (LOQ) for lignin sulfonate, and 0.5 mg L^{-1} (LOD) and 1.6 mg L^{-1} (LOQ) for humate.

Thereupon, nZVI suspensions (Fe_{tot} ~ 1 g L^{-1}) in either water type were injected. The column effluent was sampled automatically by a fraction collector every 30 s and Fe_{tot} content was quantified after acid digestion by inductively coupled plasma optical emission spectroscopy (ICP-OES, Optima 5300DV, PerkinElmer, USA).

In order to simulate the long-term effect of the modifiers application on the mobility of nZVI (after the injected modifiers in the contaminated zone are diluted by

groundwater) another 10 PVs of background solution were flushed though the columns prior to injecting the nZVI suspension.

Electric conductivity, temperature and pH of all the solutions and the nZVI suspensions were obtained in the feeding solution before and after each injection (WTW LF318 and WTW 340i, WTW Wissenschaftlich-Technische Werkstätten GmbH, Germany). Transport column experiments have been performed at least in triplicates, in order to determine the average standard deviation. Long-term transport experiments were carried out at least in duplicates. All shown breakthrough data are normalized concentrations of Fe_{tot} (C/C_0) and represent the averages.

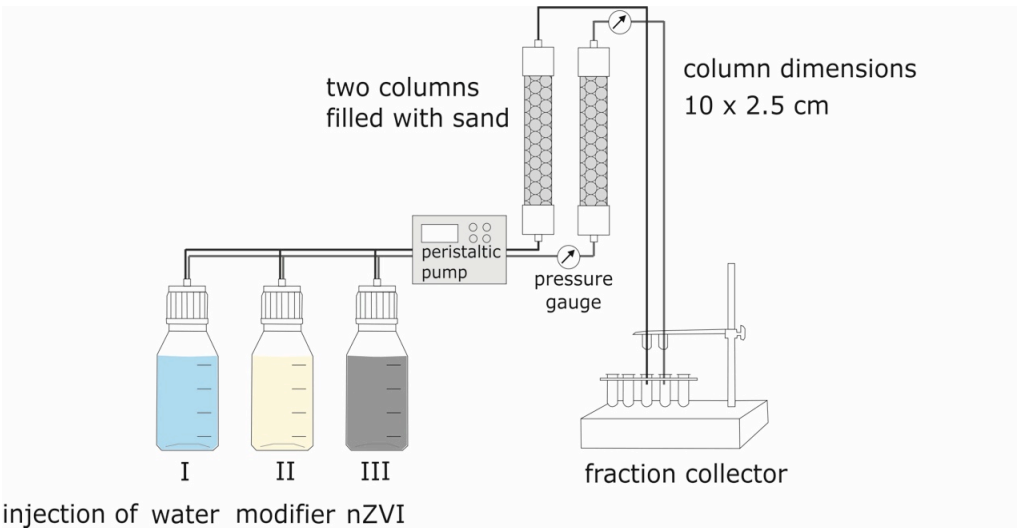

Fig. 2 — Experimental setup for column experiments; Graphic by Vesna Micić Batka.

2.7 Calculation of transport parameters following the colloid filtration theory (Elimelech et al., 1995; Kretzschmar et al., 1999; Tufenkji & Elimelech, 2004)

According to colloid filtration theory the deposition of colloids on porous media can be described with the consecutive processes of transport of particles/colloids from the fluid to the collector grains and the attachment onto those grains (Elimelech & O'Melia, 1990; Tufenkji & Elimelech, 2004). The transport of the particles is characterized by the single collector efficiency η_0, while the particles' attachment by the attachment efficiency (α) (Elimelech & O'Melia, 1990). The single collector efficiency (η_0) symbolizes the ratio of particles striking the collector to particles reaching the collector (Johnson et

al., 1996). Pursuing the approach of Tufenkji and Elimelech (2004) η_0 summarizes the mechanisms of diffusion, interception and gravitation on transport of particles. The attachment efficiency (α) represents the ratio of contacts (collisions) between colloids and grain surfaces (collector) and the culmination of actual attachments (Tufenkji & Elimelech, 2004).

Equation (1) expresses the attachment efficiency (α) following the approach of Kretzschmar et al. (1999). The parameter d_c expresses the average collector diameter [m], n the effective porosity of the sand [-], L the sand filled length of the column [m] and $\frac{C}{C_0}$ the average plateau of the breakthrough curve of Fe_{tot} in the column experiments [-].

$$\alpha = \frac{2d_c}{3(1-n)\eta_0 L} \ln\left(\frac{C}{C_0}\right) \quad (1)$$

Equation (2) affiliates the particle deposition rate coefficient (k_{CFT}) by the approach of Tufenkji and Elimelech (2004). The effective porosity of the sand is represented in (v):

$$k_{CFT} = -\frac{v}{L} \ln\left(\frac{C}{C_0}\right) = -\frac{3(1-n)}{2d_c} v\alpha\eta_0 \quad (2)$$

The theoretical transport distances (L_T) at which 99.9, 66.7 and 50% of injected particles are attached to the sand and removed (hence Fe_{tot} breakthrough is 0.001, 0.33 and 0.5) were calculated after Elimelech et al. (1995):

$$L_T = \frac{2d_c}{3(1-n)\alpha\eta_0} \ln\left(\frac{C}{C_0}\right) \quad (3)$$

2.8 Transport model

2.8.1 Modeling transport of nZVI

Additionally, the attachment and detachment transport coefficients of nZVI particles and aquifer modifiers in column experiments were modeled with a modified version of MNM1D software (Tosco & Sethi, 2010; Gastone et al., 2014) controlled with

MNMs 2015 v. 1.007 user interface (Politecnico di Torino, Italy, http://areeweb.polito.it/ricerca/groundwater/software/).

The model was calculated in one-dimensional geometry using the advection-dispersion-deposition equation (Equation (4)) with a finite-difference approach (Tosco et al., 2014). Based on the experimental data results of Fe_{tot} breakthrough, the equation was inversely solved and fitted. In Equation (4) the parameter c_{Fe} describes the breakthrough concentration observed in the experiment [g L^{-3}], ε is the effective porosity [-] obtained by the tracer test, ρ_b is the bulk density of the sand [kg m^{-3}], S_{Fe} is the total concentration of deposited particles in the column [g kg^{-1}], q represents the effective velocity [m s^{-1}] and D_x the hydrodynamic dispersion coefficient [m^2 s^{-1}], which is deduced by modeling of the conservative tracer breakthrough:

$$\frac{\partial}{\partial t}(\varepsilon c_{Fe}) + \sum_i \frac{\partial(\rho_b S_{Fe,i})}{\partial t} + \frac{\partial}{\partial x}(q c_{Fe}) - \frac{\partial}{\partial x}\left(\varepsilon D_x \frac{\partial c_{Fe}}{\partial x}\right) = 0 \qquad (4)$$

Following the approach of Tosco et al. (2014), the source and sink term (second term in Equation (4)) can be extended to take two different types of interaction sites for particle-surface-interaction into account. The modeling of nZVI transport in this study pursues this assumption and considers one site type with linear attachment/detachment kinetics and a second site type expressing non-linear kinetics such as ripening, clogging blocking and straining.

Consequently, reported output parameters for the linear kinetic site include the attachment rate $k_{a,2}$ [s^{-1}] and the detachment rate $k_{d,2}$[s^{-1}]. The output of the non-linear kinetic site is indicated by the attachment rate $k_{a,1}$[s^{-1}], the detachment rate $k_{d,1}$[s^{-1}], as well as the three dimensionless coefficients A_1 [-], B_1 [-] (both articulating the effect of deposited particles on the attachment of the non-linear kinetic site), and λ_{Fe} [-], expressing the packing of deposited iron particles on the mineral surfaces.

2.8.2 Modeling transport of aquifer modifiers

In contrast, transport models for the aquifer modifiers were computed by utilizing the one-dimensional transport equation for solutes (Equation (5); unpublished MNMs 2015 Manual; C. Bianco, personal communication, May 28, 2015) where R [-] reflects

the Retardation coefficient, C stands for the solute concentration [kg L^{-1}], D implies the dispersion coefficient [m^2 s^{-1}] and is λ the first order degradation coefficient [s^{-1}]:

$$R\frac{\partial C}{\partial t} = -v\frac{\partial C}{\partial x} + D\frac{\partial^2 C}{\partial x^2} - \lambda C \quad (5)$$

Furthermore, the definition of retardation coefficient R [-] includes the effective porosity n [-], the bulk density of the sand ρ_b [kg m^{-3}] and the soil water partition coefficient K_d [L kg^{-1}] as described in Equation (6):

$$R = 1 + \frac{\rho_b}{n}K_d \quad (6)$$

The output data for modeled transport of aquifer modifiers consists of the fitted parameters K_d, D and λ. All results computed by MNMs are derived under the assumption of perfectly homogenized sand as well as stable hydrochemical conditions.

3 Results and Discussion

3.1 Characterization of nZVI suspension

The electrophoretic mobility measurements for the nZVI suspension in MQ water revealed a particle surface ζ potential of -36.8±4.9 mV at a pH of 8.5 and an electric conductivity of 0.5 mS m^{-1} (at 25°C). The number based medium aggregate size d_{50} was 2.8 µm. Laumann et al. (2013) described NANOFER 25S suspensions as polydisperse system, derived from a broad particle size distribution. A SEM image of NANOFER S25 particles is shown in Fig. 3.

In presence of EPA water the nZVI ζ potential was reduced to -18.6±4.5 mV while medium aggregate size increased to 6.2 µm. Additionally, pH of the suspension was lowered to 7.7, reaching nearly the value for pure EPA water (7.8). The electrical conductivity increased due to the ion content in solution to 3.09 mS m^{-1} (at 25°C). The high ionic strength and divalent ion content of EPA water reduced the Debye length of the electrochemical double layer and lowered the surface charge (Sirk et al., 2009).

Moreover, the dissolved ions in solution decreased the electrostatic and repulsion between the particles, resulting in enhanced agglomeration (Saleh et al., 2008).

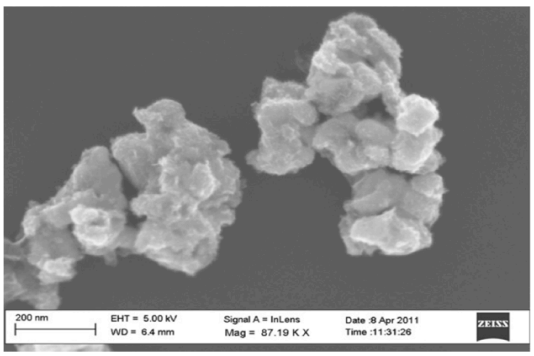

Fig. 3 – SEM image of NANOFER S25 particles; From Laumann et al. (2013).

3.2 Characterization of sand

Table 2 shows chemical properties of Dorsilit sand. According to the φ scale after Tucker (2011) (4–2 fine sand; 2–1 middle sand; 1–0 coarse sand) the sand has a mean φ of 0.78 and is therefore considered as moderately well sorted coarse sand, as shown in the sieving curve (Fig. 9A, Appendix). The tracer tests revealed an average effective porosity of 36.7%. The sands' main mineralogical component is quartz, with additional 2% of feldspar and 1% of kaolinite, as given by the producer. Chemical analysis revealed Cr (136 ppm), Ba (69 ppm) and Zr (51 ppm) as major trace elements. The TOC content undercut the LOQ of 50 ppm.

Table 2 – Chemical composition and sedimentological properties of the sand.

SiO_2	[%]	98.40	Ba	[ppm]	68.50
Al_2O_3	[%]	0.45	Co	[ppm]	<2.00
Fe_2O_3	[%]	0.17	Cr	[ppm]	135.90
CaO	[%]	<0.02	Ni	[ppm]	5.40
MgO	[%]	0.04	Sr	[ppm]	7.70
Na_2O	[%]	0.03	V	[ppm]	<5.00
K_2O	[%]	0.12	Zn	[ppm]	10.30
MnO	[%]	<0.002	Zr	[ppm]	50.90
TiO_2	[%]	0.04	TOC	[ppm]	<50.00
P_2O_5	[%]	0.009			
Sum	[%]	99.26	Effective porosity	[%]	36.70
			mean φ		0.78

3.3 Surface charge of natural sand and effect of aquifer modifiers

The ζ potential of the natural sand was analyzed in 1 mM NaCl solution and in EPA water in presence of 0, 50 and 100 mg L^{-1} of LS and HU.

The sand had a ζ potential of −43 mV at pH 5.7 in 1 mM NaCl (Fig. 4; Table 3A, Appendix). The presence of aquifer modifiers led to a decrease of ζ potential (Fig. 4). With increasing concentration to 100 mg L^{-1} LS the ζ potential of the sand decreased to −60 mV (Fig. 4a). Applying 50 mg L^{-1} HU, the ζ potential decreased to −59 mV and showed no further decrease with 100 mg L^{-1} HU (Fig. 4b).

The long-term experiments in 1 mM NaCl followed the same trends for LS and HU. Overall, a slightly less decrease of ζ potential was examined (Fig. 4) compared to the ζ potential measurements with aquifer modifier concentrations of 50 and 100 mg L^{-1}. The remaining concentration of aquifer modifiers in the system was between 5 mg L^{-1} and the LOQ (Section 3.4). The results of additional ζ potential experiments with aquifer modifier concentrations of 2 mg L^{-1} in the 1 mM NaCl solution confirmed the same decrease in ζ potential as achieved in the long-term experiments with initial higher concentrations of 50 and 100 mg L^{-1} (Table 3A, Appendix).

Changes in ζ potential of mineral surfaces are mainly influenced by pH and ionic strength of solution. Increasing concentration of aquifer modifiers in the 1 mM NaCl background solution raised the pH recorded during the measurements (Table 3A, Appendix). The recorded pH during the long-term measurements in the 1mM NaCl system was nearly equal compared to the pure background solutions (Table 3A, Appendix). Previous publications revealed a relative constant ζ potential of quartz sand in the relevant pH range researched in this study between 5.5 and 9 (Chibowski 1979; Laumann et al., 2013). In addition, elevated ionic strength induces a compression of the electronic double layer, leading to an increase of ζ potential (Revil et al., 1999). Consequently, the significant decrease of ζ potential in the 1 mM NaCl solution can be adjudged to the interactions of the sand with polyelectrolytes and indicates that the aquifer modifiers could be adsorbed to the mineral surfaces of quartz sand. Low sorption of LS and HU onto quartz-rich material has been demonstrated by Grigg and Bai (2004) and Pitois et al. (2008).

The ζ potential of the sand in EPA water was more positive with −25 mV at a pH of 8.0. This can be attributed to the high ionic strength of EPA water (5.5 mM), as well as

specific adsorption of Ca^{2+} and Mg^{2+} on the mineral's surface leading to a decrease of surface potential (Breeuwsma & Lyklema, 1972; Laumann et al., 2014).

In presence of the aquifer modifiers in EPA water, all the ζ potential measurements were equal to those in pure EPA solution or varied in the error range ± 3 mV, with pH values of 8.1–8.4.

The long-term effect measurements in EPA water showed similar ζ potentials of the sand to that in pure EPA water. Besides the effect of higher ionic strength on surface potential, positively charged divalent cations could attach onto negatively charged groups of polyelectrolyte molecules, thus lowering their ability to adsorb onto mineral surfaces (Vermöhlen et al., 2000) and reducing the negative charge of the aquifer modifier molecules. Furthermore, the addition of higher concentrations of modifiers also increases the ionic strength of the solution.

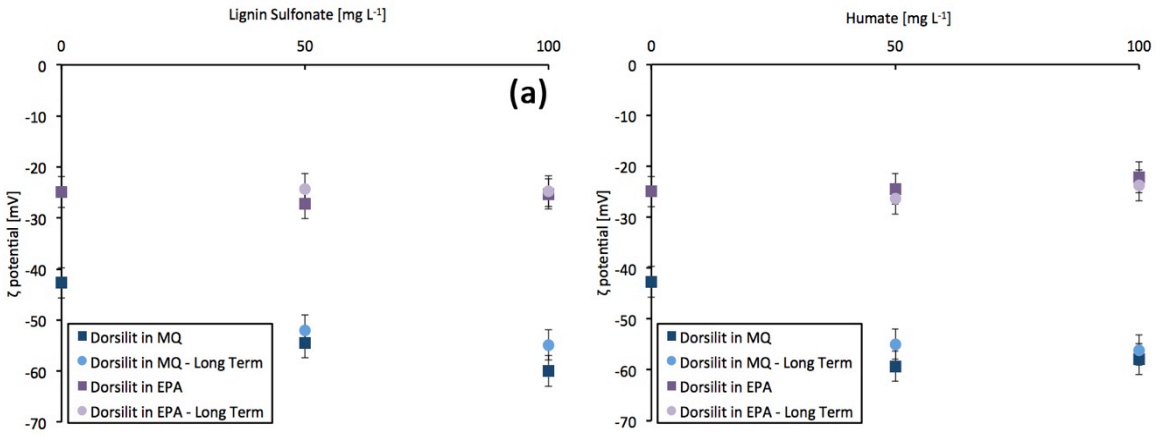

Fig. 5 – ζ potential of quartz sand as a function of (a) lignin sulfonate and (b) humate concentration in MQ and EPA background solution. Results of long-term experiments are plotted with their initial concentration of aquifer modifiers.

3.4 Interaction between aquifer modifiers and granular matrix

In order to evaluate the interactions between aquifer modifiers and sand, solutions of either LS or HU were firstly injected into columns.

The breakthrough curves (C/C_0) of both aquifer modifiers were lagged in relation to the bromide tracer (Fig. 5a) and reached one ($C/C_0 = 1$) after ca. 3 PVs (Fig. 5a). The short lag between the breakthrough of the tracer and the modifiers is considered to result from sparse interaction of the aquifer modifier molecules with the sand surface.

The breakthrough curves in Fig. 5a indicate an earlier elution of modifiers than the tracer. This can be attributed to the size exclusion effect, resulting from bigger sized aquifer modifier molecules being excluded from small pore pores, hence travelling faster in the streamlines of well connected pore spaces. In contradiction, the conservative Br^- Ions of the tracer are considered to travel through the whole effective pore space of the column.

Furthermore, the MNMs modeling coefficients of the aquifer modifiers breakthrough were determined. The fitted coefficients for HU and LS were similar in both water types. The dispersivity D [m] ranged between 1 x 10^{-5} and 2 x 10^{-3}, whereas the soil-water partition coefficient K_d [L kg^{-1}] varied between 1.8 x 10^{-4} and 2.2 x 10^{-4} (Table 6A, Appendix). The model was run by setting the first order degradation rate λ [s^{-1}] = 0 since no degradation of the aquifer modifiers was assumed during the experiments

In order to further assess the behavior of modifiers, the columns were flushed with pure background solution after the aquifer modifier injection while the effluents were sampled and analyzed (Fig. 5b). The results demonstrated that after only 2 PVs >80% of modifiers was recovered (Fig. 5b). After 10 PVs the remaining amount of modifiers was recovered, exception of HU solution in EPA water, which breakthrough remained close to 0.1, which indicated perhaps an irreversible interaction with mineral grains (Fig 5b).

Since detailed molecular analysis is absent by the producers of the both aquifer modifiers, there is lack of information which fraction of LS and HU could be adsorbed to the mineral surfaces during the experiments. Molecules of humic acid have a bigger size distribution compared to LS (Section 2.2). The content and ratio of functional groups of LS and humic acid molecules depend on their molecular weight (Collins et al., 1986; Kim et al., 1990; Yang et al., 2007). It assumed, that the low molecular weight fractions of both aquifer modifiers are more reactive and preferentially adsorbed (Glasser et al., 1974; Pitois et al., 2008).

Literature reports little sorption of humic acid on negative charged quartz surfaces (Johnson et al., 2009). Grigg and Bai (2004) demonstrated sorption of lignin sulfonate on sandstone, Laumann et al. (2014) did not detect any sorption of LS on round shaped, acid-washed standard Ottawa quartz sand. The natural sand used in the experiments is mainly consisting of quartz minerals, therefore the low sorption of the aquifer modifiers

onto quartz rich natural sand is in agreement with the assumption of electrostatic repulsion of negatively charged polyelectrolytes on negatively charged quartz surfaces.

The interaction between HU and the sand in EPA water could be a result of Ca^{2+} bridging between the negatively charged humic acid molecules and the negative charged sand surface. Previous research demonstrated that carboxylic groups of humic acid have an affinity to interact with Ca^{2+} (Chen et al., 2007b; Jada et al., 2006; Li & Elimelech, 2004). Bridging effects of humic acid molecules in presence of Ca^{2+} were reported in Literature (Dong & Lo, 2013b; Chen et al., 2007b; Liu et al., 2011; Jada et al. 2006; Laumann et al., 2014). Further, Jada et al. (2006) proved sorption of humic acid onto quartz sand particles in presence of Ca^{2+} and increased ionic strength. Hence, it is presumed that Ca^{2+} ions bridges between carboxylic groups of the humic acid molecules and the hydroxyl groups at the mineral's surface. As LS was faster recovered than HU in EPA water (Fig. 5b), it is assumed that the LS used in this study bears less carboxylic content than the humic acid molecules of HU.

It is hypothesized that the natural sand could act as a filter during the modifier injections and strongly adsorbs the most reactive molecule fractions of the modifiers to its mineralogical and chemical impurities. MNMs software failed to fit breakthrough of flushed modifiers applying a finite-different approach that includes fitting dispersivity coefficient D and soil-water partition coefficient K_d.

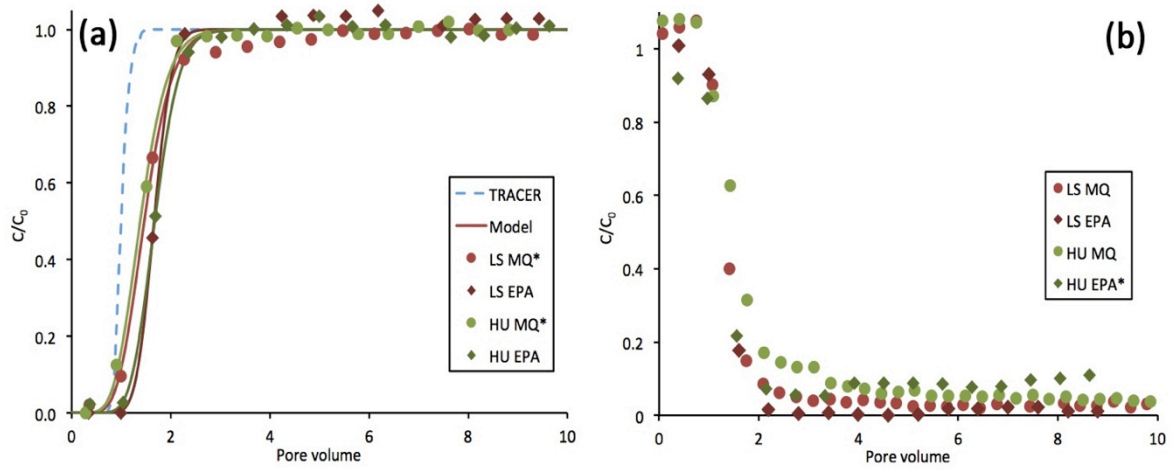

Fig. 6 – Aquifer modifier breakthrough C/C_0 in MQ and EPA water (a) during injection into the column (initial concentration of 100 mg L^{-1}) and (b) during flushing the column with background solution after aquifer modifier injection (initial aquifer modifier concentration of 50 mg L^{-1}). Solid lines represent the modeled modifier breakthrough, applying MNMs model. The dashed line illustrates the modeled breakthrough of the conservative tracer. Fluid velocity was kept constant at 100 m d^{-1}. The plotted experimental values of injection 100 mg L^{-1} LS in MQ, 100 mg L^{-1} HU in MQ and the column flushing with 50 mg L^{-1} HU in EPA water were provided by Doris Schmid (*).

3.5 Effect of pre-injected aquifer modifiers on nZVI transport

The pH and EC of all nZVI feeding-suspensions were consistent before start and after end of injections in both waters. Moreover, the pressure gradient between in- and outlet of the column stayed constant during all experiments (data not shown).

All Fe_{tot} breakthrough curves were retarded compared to that of the tracer, indicating nZVI deposition onto the mineral grains (Fig. 6a-d). The shape of the nZVI breakthrough curves showed an initial maximum peak, after which breakthrough slowly decreased. Tosco et al. (2014) described this phenomenon as filter ripening, resulting of non-linear deposition, which occurs if particles are irreversibly attached to the sand.

The attached nZVI particles contribute supplementary collector surface and increase particle removal from the suspension (Kretzschmar et al., 1995), resulting in formation of multilayer particle deposits on the grain surface (Liu et al., 1995).

With pre-injection of aquifer modifiers the maximum peak of breakthrough arose prior compared to the pure background solution transport experiments. The high concentration of polyelectrolytes in the pore water after the pre-injection of the aquifer modifier could possibly stabilize the first fraction of injected nZVI particles and therefore enhance their mobility. Literature has proven that negatively charged polyelectrolytes are able to stabilize nZVI particles (Phenrat et al., 2008) and consequently promote their transport (Laumann et al., 2014; Johnson et al., 2009).

The model fitting implies that the size exclusion effect was also noticeable in the Fe_{tot} breakthrough in modified sand. In contradiction to the completely soluble Br^- anions of the conservative tracer, the travel paths of the larger nZVI particles exclude small pore spaces, which results to a prior nZVI elution compared to the tracer (Kretzschmar et al., 1997; Section 3.4).

Solutions of both aquifer modifiers had different effects on nZVI transport, depending on the type of water they were prepared in. The nZVI in MQ in not modified sand reached an average breakthrough plateau of C/C_0 (Fe_{tot}) = 0.32. The pre-injection of LS and HU in concentrations of 50 and 100 mg L^{-1} in MQ water appear to have no effect on the nZVI mobility under these conditions, considering the widespread relative standard deviations (Fig. 6a & b).

The nZVI particles were practically immobile in the divalent cation-rich EPA in non-modified sand. In EPA water nZVI particles are fairly large (6.2 µm). As a result of the increased aggregate size and reduced surface charge of nZVI in EPA water, the attachment to the mineral grains increased. Therefore, the large nZVI aggregate fraction may be filtered in the first three cm of the columns near the inlet, which deployed an intensive black colored zone. The breakthrough was 0.05, approaching nearly zero at the end of nZVI injection. After injected 10 PVs, the color of the effluent was clear translucent yellow, indicating presence of oxidized iron particles. Analyses of these oxidized particles revealed a considerably smaller average aggregate size of 251 nm and a ζ potential of −26±4.6 mV. Since the total iron content was detected in the effluent after acidic dissolution, the minor amount of the small oxidized iron particles was included in the value, leading to a Fe_{tot} breakthrough >0.

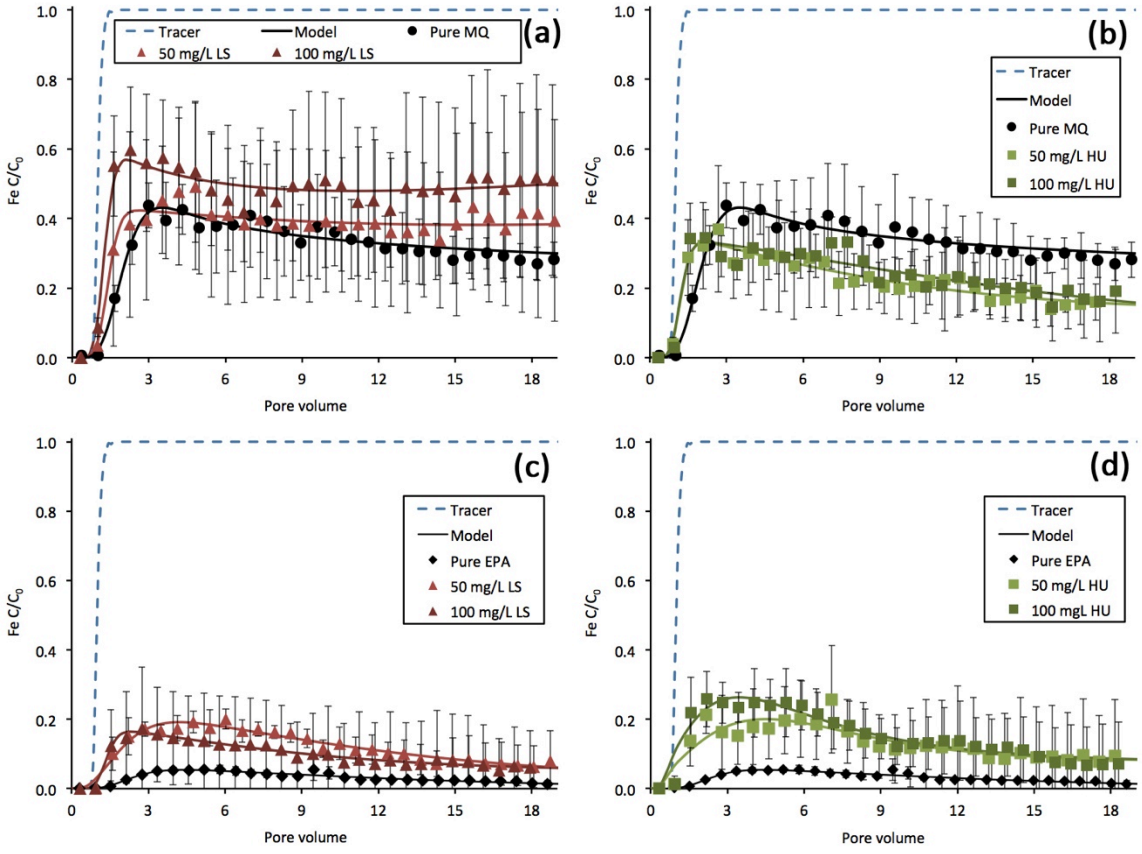

Fig. 7 – Total iron breakthrough as a function of concentration of pre-injected lignin sulfonate and humate in MQ (a,b) and EPA water (c,d). nZVI transport models calculated by MNMs are represented as solid lines, the dashed line highlights the conservative tracer model. All data obtained, performed and provided by Doris Schmid except experiments in pure MQ and EPA water.

The nZVI transport in EPA water was enhanced after the injection of HU into sand. Pre-injected HU increased the average Fe_{tot} plateau-breakthrough from 0 to ca. 0.2 for both HU concentrations applied (50 and 100 mgL^{-1}, Fig. 6). The utilization of LS in EPA water highlighted high standard deviations and presumably failed in enhancing the nZVI (Fig. 6).

Additionally, floccules of aquifer modifiers could conceivably interact with nZVI particles. Hence, size and characteristics of possible aquifer modifier floccules must be analyzed under different aquifer modifier concentrations.

3.6 Long-term effect of pre-injected aquifer modifiers on nZVI transport

In order to elucidate if the modification of aquifer may have a longer effect on nZVI transport, after a modifier is possibly diluted with groundwater and nZVI is re-injected a set of transport experiments was performed, including (i) pre-injection of modifier, (ii) column flushing with a background solution and (iii) injection of nZVI. The pressure gradient between column in- and outlet was constant during all experiments (data not shown). The experimental results are shown in Fig. 7a-d. Modifiers concentrations of 50 and 100 mg L^{-1} refer to the concentrations of the initially injected modifier before the flushing with 10 PVs of the background solutions.

All long-term transport experiments were performed in duplicates; accordingly the experimental data lacks standard deviations (Fig. 7) and has to be critically interpreted. The experiments conducted with initially 100 mg L^{-1} of aquifer modifiers increased the nZVI transport independently of type of water the experiment was conducted in (Fig. 7). In contrast, all experiments run with initially 50 mg L^{-1} of LS and HU resulted in similar nZVI transport like to the injection of nZVI only (Fig. 7). The resulting constant breakthrough of 0.05 in EPA water when applying 50 mg L^{-1} of LS and HU is estimated to result from enhanced transport of a small fraction of small oxidized iron particles, as mentioned in Section 3.5. When applying 100 mg L^{-1}, conversely, the dark color of nZVI suspension was observed in the column effluents, indicating the presence of nZVI. The results might indicate, that HU has superior potential to enhance long-term nZVI transport than LS.

This demonstrates that even small amount of modifiers, which remained in the column after it was flushed with the background solution (possibly <5 mg L^{-1}), could be

sufficient to enhance transport of nZVI, independent of the type of water the experiments were conducted in. The potential of lower concentrations of modifiers to promote transport of nZVI remains to be explored in future studies.

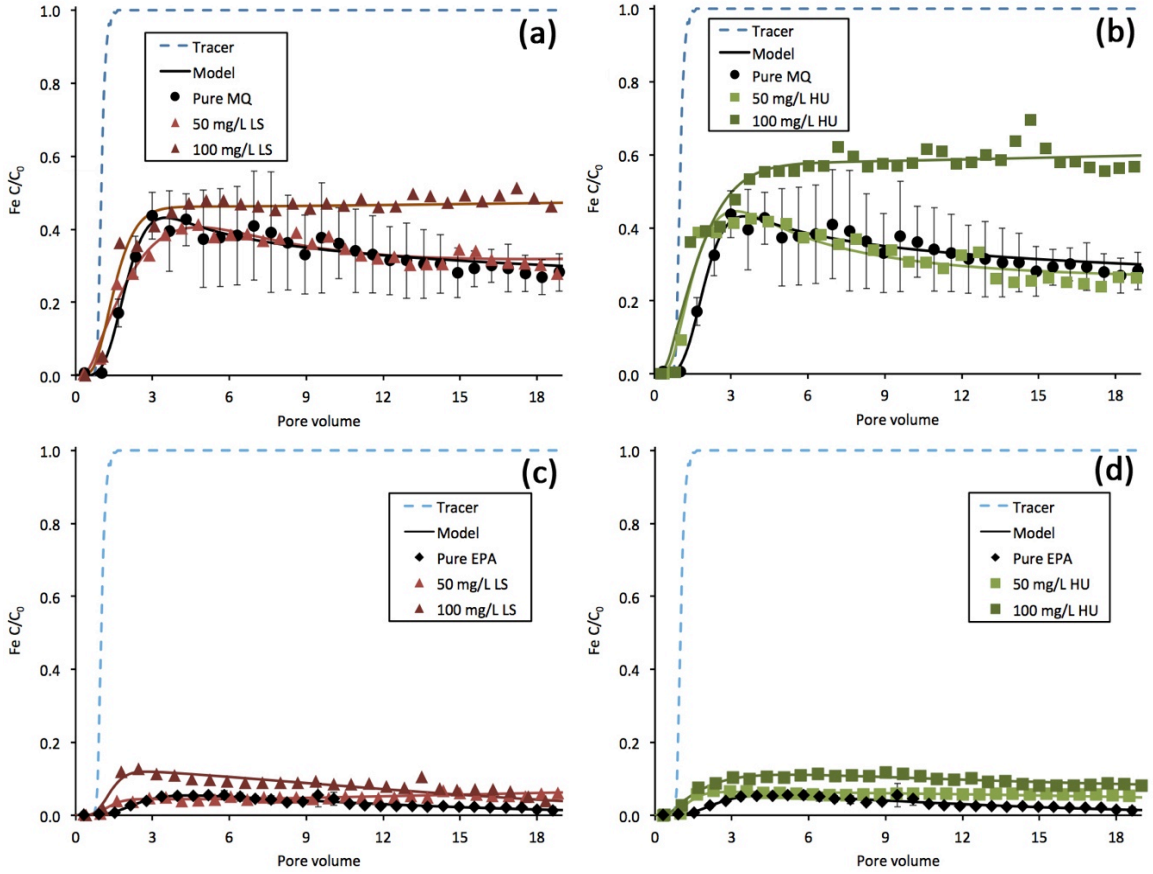

Fig. 8 – Total iron breakthrough in long-term transport experiments as a function of concentration of pre-injected lignin sulfonate and humate in MQ (a,b) and EPA water (c,d) prior to flushing with background solution. nZVI transport models calculated by MNMs are represented as solid lines, the dashed line highlights the conservative tracer model.

In the MQ water pre-injected aquifer modifiers could have increased nZVI transport in the long-term transport experiments, whereas this effect was absent in the transport experiments described in Section 3.5. Concerning those discrepancies between breakthrough in transport (Section 3.5) and long-term transport experiments (Section 3.6), following points should be considered.

(1) A fine, white colored fraction of the sand, seen in Fig. 10A (Appendix), was flushed out of the column during the flushing step (with background solutions) in the long-term transport experiment. It is likely that aquifer modifier possibly mobilized the fine sand fraction. This could have slightly increased the porosity, lowered collector

surface and provided additional pathways for nZVI through the granular matrix. As no flushing was performed before the nZVI injection in the transport experiments described in Section 3.5, the fine sand fraction likely remained in the column and could has hetero-aggregated with nZVI particles. Hetero-aggregates are considered bigger sized and less mobile than nZVI, therefore contributing additional attachment surface in the pore space and further clogging transport pathways

(2) Detailed analyses of the aquifer modifiers' molecular structure and molecular weight were not provided and are needed to shed light on their sorption and interaction characteristics. Further transport experiments with lower aquifer modifier concentrations without the flushing step are necessary to fully assess mobility behavior of nZVI after pre-injection of aquifer modifiers.

3.7 Calculated parameters and model coefficients of nZVI transport

Colloid filtration theory assumes particles and collector grains as perfectly round shaped and uniform sized (Tufenkji & Elimelech, 2004; Yao et al., 1971). Moreover, the particle breakthrough is presumed to reach a constant plateau during the whole injection. It has to be considered that the sand used in this study as well as the nZVI particles used show variations in shape and grain size (Section 3.1; Fig. 9A, Appendix) and the Fe_{tot} breakthrough curves vary in shape. Further, increased values of average Fe_{tot} plateau-breakthrough fail to state enhancement of nZVI transport values if taking high standard deviations into account (Section 3.5 and 3.6). Therefore, the resulting model data have to be regarded critically.

Fig. 8 highlights the trend lines for the maximum theoretical transport distances $L_{T\ 0.001}$ of nZVI in the MQ and EPA water. The maximum calculated $L_{T\ 0.001}$ of 0.99 m was attained with pre-injection of 100 mg L^{-1} LS, representing with the highest reached average plateau-breakthrough in MQ. Despite the theoretical $L_{T\ 0.001}$ in EPA water was increased from 0.20 to 0.37 m (100 mg L^{-1} HU), nZVI was immobile in EPA water without pre-injection of aquifer modifiers (see Section 3.5).

Transport distance increases if attachment efficiency α and the first order removal rate k_{CFT} decrease. The increase of mean particle diameter due to the ionic content of solution induces a higher single collector efficiency η_0 for nZVI transport in EPA

water (0.09) compared to MQ (0.02; Table 4A, Appendix). Subsequently, the steepness of the transport distance trend lines in Fig.8 is a function of particle size.

Following the MNMs modeling approach of Tosco et al. (2014), the coefficient A_1 [-] of the non-linear term in the advection-dispersion-deposition equation was assumed to be positive for all experiments at a value of 1000 (Table 4A, Appendix). This indicates clogging of active sites and leads to an increasing deposition rate with increasing iron concentration in the sand.

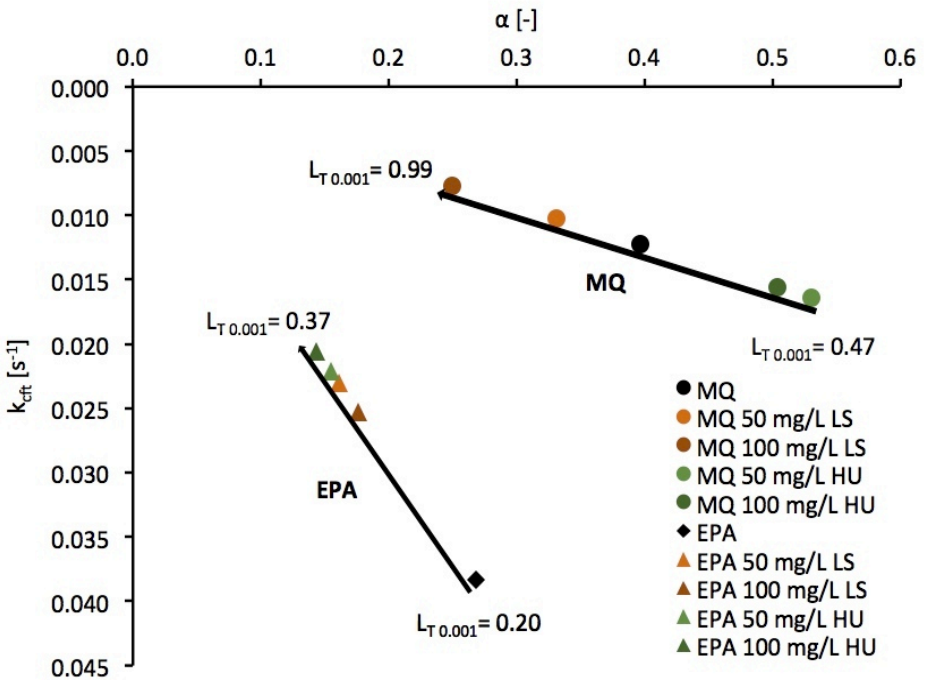

Fig. 9 – Increase of theoretical maximal transport length $L_{T\,0.001}$ [m] of nZVI as a function of first order removal rate k_{CFT} and the attachment efficiency α in MQ and EPA water.

Referring to the model data, attachment and detachment in the sand filled column was dominated by the kinetics of the linear reaction site $k_{a,2}$ and $k_{d,2}$ (Table 4A, Appendix). All other modeled coefficients varied strong between each injection model in both water types. Consequently, the contradictory model coefficient data lacked trends with the iron breakthrough data. As a result, expected correlation between the highest attachment rate k_a for each breakthrough with the first order removal rate k_{CFT} calculated after the colloid filtration theory is absent (Table 4A, Appendix). In addition, it is worth to mention that MNMs software includes the single collector

efficiency η_0 following the contrasting approach of Messina et al. (2015) in the model calculations.

The broad spread of modeled coefficients could be elucidated by the altering geometry of the breakthrough curves. Differing shapes of the breakthrough curves are expected to produce varying model coefficients of the non-linear-attachment-term of the transport equation used for the simulation (Section 2.8; Table 5A, Appendix). Model data of the relatively uniformly shaped breakthrough curves of the long-term transport experiments exhibits consensus in certain coefficients (Table 4A, Appendix). If nZVI breakthrough was enhanced in MQ, the attachment rate $k_{a,1}$ and the ripening exponent B_2 decreased while detachment rate $k_{d,2}$ increased. Additionally, long-term experiments in EPA water show a correlation between raised nZVI breakthrough and decrease of $k_{a,1}$.

4 Conclusions and implications for field injection

The experimental data of this study indicate that pre-injection of negatively charged polyelectrolytes, namely lignin sulfonate and humate in quartz sand has a potential to improve nZVI mobility under well-controlled laboratory conditions.

The ζ potential of quartz sand could be reduced and permanently lowered with aquifer modifiers in ultrapure MQ water. Detectable change of ζ potential in the high ionic strength EPA water was absent. Additionally, divalent cation rich EPA water increased the ζ potential of the coated nZVI particles, resulting in reduced electrostatic and electrosteric repulsion between the particles. Consequently, the average aggregate size increased, making the particles practically immobile in EPA water without pre-injection of aquifer modifiers. This effect is expected to also occur at *in situ* conditions injections in the natural environment.

The smallest fraction of nZVI particles, which is expected to be transported most further from the injection point may be oxidized, therefore having lower reactivity towards contaminants. Hence, the reactivity of nZVI has to be examined in parallel with its mobility and both critically evaluated before designing larger scale experiments or field application.

The transport coefficients calculated after colloid filtration theory proofed an increase in maximum theoretical transport distance $L_{T\ 0.001}$ of nZVI while attachment efficiency and the first order removal rate decrease, after aquifer modification. It should be noted that shape and size distribution of the sand grains and nZVI particles used in the experiments show variations from the initial assumptions of the colloid filtration theory. Moreover, the resulting values are derived from well-controlled small-scale laboratory experiments, which simplify the full complexity encountered at actual field sites. Consequently, research of aquifer modification in large scale experiments will be necessary before applying this potential technology in field sites.

During the transport experiments it has been demonstrated that solutions both modifiers showed different influence on nZVI transport, depending on the water type they are prepared in. Pre-injection of aquifer modifiers induced no effect on nZVI transport in the MQ water. Applied in EPA water, humate increased the breakthrough. Conducted in a concentration of 100 mg L^{-1}, the maximal theoretical transport distance $L_{T\ 0.001}$ was increased to 37 cm. In addition, long-term transport experiments may indicate that humate has potential of prolonged enhancement of nZVI mobility. Therefore, humate is considered to be the preferential aquifer modifier under natural conditions.

Accordingly, to ensure a complete insight of the aquifer modification effects and processes revealed by lignin sulfonate and humate, detailed analysis of this polyelectrolytes and additional transport experiments applying lower concentrations of modifiers are necessary.

In order to distribute nZVI properly in the contaminated field site, further improvement of transport will be inevitably since the ionic strength in contaminated groundwater can exceed that of EPA water. In addition, in most cases real aquifer material contains higher proportions of chemical and mineralogical heterogeneities, providing positively charged collector sites, which can enhance attachment of nZVI and results in reduced transport. In order to obtain maximum effect of aquifer modification under natural conditions for remediation, detailed investigations with site-specific hydrochemistry and aquifer material are needed. Moreover, possible interactions between aquifer modifiers and contaminants remain to be investigated, as well as their influence on nZVI reactivity and finally the effects they may exhibit to ingenuous

microorganisms. Only after a critical evaluation of all the effects and benefits of the aquifer modification, it can be decided if this approach is beneficial for *in situ* remediation.

As the transport of nZVI in calcium rich water can be improved if the particles are co-injected with polyelectrolytes (Laumann et al., 2014), it is worth of considering a combined pre- and co-injection of modifiers in order to maximally promote the mobility of nZVI under this conditions.

5 Acknowledgements

This research received funding from the European Union's Seventh Framework Programme FP7/2007-2013 under grant agreement n°309517.

I particularly thank Dr. Vesna Micić Batka and Doris Schmid for prosperous discussions, support and feedback.

I especially thank Univ. Prof. Dr. Thilo Hofmann for his supervision and feedback.

Thanks to my family, friends and labmates for being my constant source of encouragement and motivation.

6 References

Awungacha Lekelefac, C., Hild, J., Czermak, P., & Herrenbauer, M. (2014). Photocatalytic active coatings for lignin degradation in a continuous packed bed reactor. *International Journal of Photoenergy, 1* (1), 1–6.

Beckett, R., Jue, Z., Giddings, J. C. (1987). Determination of molecular weight distributions of fulvic and humic acids using Field-Flow Fractionation. *Environmental Science & Technology, 21* (3), 289–295.

Borkovec, M., & Papastavrou, G. (2008). Interactions between solid surfaces with adsorbed polyelectrolytes of opposite charge. *Current Opinion in Colloid & Interface Science, 13* (6), 429–437.

Breeuwsma, A., & Lyklema, J. (1973). Physical and chemical adsorption of ions in the electrical double layer on hematite (α-Fe2O3). *Journal of Colloid and Interface Science, 43* (2), 437–448.

Chang, M. C., & Kang, H. Y. (2009). Remediation of pyrene-contaminated soil by synthesized nanoscale zero-valent iron particles. *Journal of Environmental Science and Health Part A, 44* (6), 576–582.

Chen, J., Xiu, Z., Lowry, G. V., & Alvarez, P. J. (2011). Effect of natural organic matter on toxicity and reactivity of nano-scale zero-valent iron. *Water Research, 45* (5), 1995–2001.

Chen, K. L., Mylon, S. E., & Elimelech, M. (2007a). Enhanced aggregation of alginate-coated iron oxide (hematite) nanoparticles in the presence of calcium, strontium, and barium cations. *Langmuir, 23* (11), 5920–5228.

Chen, K. L., & Elimelech, M. (2007b). Influence of humic acid on the aggregation kinetics of fullerene (C_{60}) nanoparticles in monovalent and divalent electrolyte solutions. J*ournal of Colloid and Interface Science, 309* (1), 126–134.

Chibowski, E. (1979). Zeta potential and surface free energy changes: Quartz/n-heptane-water system. *Journal of Colloid and Interface Science, 69* (2), 326–329.

Chowdhury, I., Cwiertny, D. M., & Walker, S. L. (2012). Combined factors Influencing the aggregation and deposition of nano-TiO 2 in the presence of humic acid and bacteria. *Environmental Science & Technology, 46* (13), 6968–6976.

Collins, M. R., Amy, G. L., & Steelink, C. (1986). Molecular weight distribution, carboxylic acidity, and humic substances content of aquatic organic matter: Implications for removal during water treatment. *Environmetal Science & Technology, 20* (10), 1028–1032.

Conte, P., Agretto, A., Spaccini, R., & Piccolo, A. (2005). Soil remediation: humic acids as natural surfactants in the washings of highly contaminated soils. *Environmental Pollution, 135* (3), 515–522.

Crane, R. A., & Scott, T. B. (2012). Nanoscale zero-valent iron: future prospects for an emerging water treatment technology. *Journal of Hazardous materials, 211*, 112–125.

Crane, R., Dickinson, M., Popescu, I., & Scott, T. (2011). Magnetite and zero-valent iron nanoparticles for the remediation of uranium contaminated environmental water. *Water Research, 45* (9), 2931–2942.

Dobrynin, A. V., & Rubinstein, M. (2005). Theory of polyelectrolytes in solutions and at surfaces. *Progress in Polymer Science, 30* (11), 1049–1118.

Dong, H., & Lo, I. M. (2013a). Influence of humic acid on the colloidal stability of surface-modified nano zero-valent iron. *Water Research, 47* (1), 419–427.

Dong, H., & Lo, I. M. (2013b). Influence of calcium ions on the colloidal stability of surface-modified nano zero-valent iron in the absence or presence of humic acid. *Water Research, 47* (7), 2489–2496.

Elimelech, M., & O'Melia, C. R. (1990). Kinetics of deposition of colloidal particles in porous media. *Environmental Science & Technology, 24* (10), 1528–1536.

Elimelech, M., Gregory, J., & Jia, X. W. (1995). *Particle depositon and aggregation: Measurement, modeling and simulation.* Oxford: Butterworth-Heinemann.

Fairbrother, F., & Mastin, H. (1924). CCCXII.–Studies in electro-endosmosis. Part I. *Journal of the Chemical Society, Transactions, 125*, 2319–2330.

Gastone, F., Tosco, T., & Sethi, R. (2014). Guar gum solutions for improved delivery of iron particles in porous media (Part 1): Porous medium rheology and guar gum-induced clogging. *Journal of Contaminant Hydrology, 166*, 23–33.

Glasser, W., Gratzl, J., Forss, K., Hrutfiord, B., Johanson, L., McCarthy, J., & Collins, J. (1974). *Studies of Low Molecular weight Lignin Sulfonates. Project 12040 DEH, EPA-660/2-74-069.* Washington, D.C.: Pacific Northwest Environmental Research Laboratory, National Environmental Research Center, U. S. Environmental Protection Agency

Grieger, K. D., Fjordbøge, A., Hartmann, N. B., Eriksson, E., Bjerg, P. L., & Baun, A. (2010). Environmental benefits and risks of zero-valent iron nanoparticles (nZVI) for in situ remediation: risk mitigation or trade-off? *Journal of Contaminant Hydrology*, *118* (3), 165–183.

Grigg, R. B., & Bai, B. (2004). Calcium lignosulfonate adsorption and desorption on Berea sandstone. *Journal of Colloid and Interface Science, 279* (1), 36–45.

Hofmann, T., & Von der Kammer, F. (2009). Estimating the relevance of engineered carbonaceous nanoparticle facilitated transport of hydrophobic organic contaminants in porous media. *Environmental pollution, 157* (4), 1117–1126.

Hunter, R. J. (1988). *Zeta potential in Colloid Science. Principles and Application.* London, UK: Academic Press.

Jada, A., Ait Akbour, R., & Duch, J. (2006). Surface charge and adsorption from water onto quartz sand of humic acid. *Chemosphere, 64* (8), 1287–1295.

Jiemvarangkul, P., Zhang, W. X., & Lien, H. L. (2011). Enhanced transport of polyelectrolyte stabilized nanoscale zero-valent iron (nZVI) in porous media. *Chemical Engineering Journal, 170* (2), 482–491.

Johnson, P. R., Sun, N., & Elimelech, M. (1996). Colloid transport in geochemically heterogeneous porous media: modelling and measurements. *Environmental Science & Technology*, *30* (11), 3284–3293.

Johnson, R. L., Johnson, G. O., Nurmi, J. T., & Tratnyek, P. G. (2009). Natural organic matter enhanced mobility of nano zerovalent iron. *Environmental Science & Technology, 43* (14), 5455–5460.

Jones, E. H., & Su, C. (2012). Fate and transport of elemental copper (Cu 0) nanoparticles through saturated porous media in the presence of organic materials. *Water Research, 46* (7), 2445–2456.

Juhl, K., Pedersen, C., Bovet, N., Dalby, K., Hassenkam, T., Andersson, M., Okhrimenko, D.V., & Stipp, S. L. S. (2014). Adhesion of alkane as a functional group on muscovite and quartz: Dependence on pH and contact time. *Langmuir, 30* (48), 14476–14485.

Kadar, E., Tarran, G. A., Jha, A. N., & Al-Subiai, S. N. (2011). Stabilization of engineered zero-valent nanoiron with Na-acrylic copolymer enhances spermiotoxicity. *Evironmental Science & Technology, 45* (8), 3245–3251.

Kanel, S. R., Manning, B., Charlet, L., & Choi, H. (2005). Removal of arsenic (III) from groundwater by nanoscale zero-valent iron. *Environmental Science & Technology, 39* (5), 1291–1298.

Karn, B., Kuiken, T., & Otto, M. (2009). Nanotechnology and in situ remediation: a review of the benefits and potential risks. *Environmental health perspectives, 117*, 1823–1831.

Keller, A. A., Garner, K., Miller, R. J., & Lenihan, H. S. (2012). Toxicity of nano-zero valent iron to freshwater and marine organisms. *PloS one, 7* (8), e43983.

Kim, H. J., Phenrat, T., Tilton, R. D., & Lowry, G. V. (2012). Effect of kaolinite, silica fines and pH on transport of polymer-modified zero valent iron nano-particles in heterogeneous porous media. *Journal of colloid and interface science, 370* (1), 1–10.

Kim, J. I., Buckau, G., Li, G. H., Duschner, H., & Psarros, N. (1990). Characterization of humic and fulvic acids from Gorleben groundwater. *Fresenius' Journal of Analytical Chemistry, 338* (9), 245–252.

Kretzschmar, R., Robarge, W. P., & Amoozegar, A. (1995). Influence of organic matter on colloid transport through saprolite. *Water Resources Research, 31* (3), 435–445.

Kretzschmar, R., & Sticher, H. (1997). Transport of humic-coated iron oxide colloids in a sandy soil: Influence of Ca^{2+} and trace metals. *Environmental Science & Technology, 31* (12), 3497–3504.

Kretzschmar, R., Borkovec, M., Grolimund, D., & Elimelech, M. (1999). Mobile subsurface colloids and their role in contaminant transport. *Advances in agronomy*, *66*, 121–193.

Laumann, S., Micić Batka, V., & Hofmann, T. (2014). Mobility enhancement of nanoscale zero-valent iron in carbonate porous media through co-injection of polyelectrolytes. *Water research, 50*, 70–79.

Laumann, S., Micić Batka, V., Lowry, G. V., & Hofmann, T. (2013). Carbonate minerals in porous media decrease mobility of polyacrylic acid modified zero-valent iron nanoparticles used for groundwater remediation. *Environmental Pollution, 179*, 53–60.

Le Bell, J. (1984). The relation between the structure of lignosulphonates and their effect as stabilizers for latex particulate dispersions. *Colloids and Surfaces, 9* (3), 237–251.

Lerner, R. N., Lu, Q., Zeng, H., & Liu, Y. (2012). The effects of biofilm on the transport of stabilized zerovalent iron nanoparticles in saturated porous media. *Water Research, 46* (4), 975–985.

Lewis, J., & Sjöstrom, J. L. (2010). Optimizing the experimental design of soil columns in saturated and unsaturated transport experiments. *Journal of Contaminant Hydrology, 115* (1-4), 1–13.

Li, Q., & Elimelech, M. (2004). Organic fouling and chemical cleaning of nanofiltration membranes: Measurements and mechanisms. *Environmental Science & Technology, 38* (17), 4683–4693.

Li, X. Q., & Zhang, W. X. (2007). Sequestration of metal cations with zerovalent iron nanoparticles a study with high resolution X-ray photoelectron spectroscopy (HR-XPS). *The Journal of Physical Chemistry C, 111* (19), 6939–6946.

Liu, D., Johnson, P. R., & Elimelech, M. (1995). Colloid deposition dynamics in flow through porous media: Role of electrolyte concentration. *Environmental Science & Technology, 29* (12), 2963–2973.

Liu, X., Wazne, M., Chou, T., Xiao, R. & Xu, S. (2011). Influence of Ca^{2+} and Suwannee River Humic Acid on aggregation of silicon nanoparticles in aqueous media. *Water Research, 45* (1), 105–112.

Messina, F., Marchisio, D., & Sethi, R. (2015). An extended and total flux normalized correlation equation for predicting single-collector efficiency. *Journal of Colloid and Interface Science, 446*, 185–193.

Milczarek, G., Rebis, T., & Fabianska, J. (2013). One-step synthesis of lignosulfonate-stabilized silver nanoparticles. *Colloids and Surfaces B: Biointerfaces, 105*, 335–341.

Moacanin, J., Felicetta, V. F., Haller, W., & McCarthy, J. L. (1955). Lignin. VI. Molecular weight of lignin sulfonates by light scattering. *Journal of the American Chemical Society, 77* (13), 3470–3475.

Phenrat, T., Saleh, N., Sirk, K., Kim, H. J., Tilton, R. D., & Lowry, G. V. (2008). Stabilization of aqueous nanoscale zerovalent iron dispersions by anionic polyelectrolytes: adsorbed anionic polyelectrolyte layer properties and their effect on aggregation and sedimentation. *Journal of Nanoparticle Research, 10* (5), 795–814.

Phenrat, T., Kim, H. J., Fagerlund, F., Illangasekare, T., Tilton, R. D., & Lowry, G. V. (2009). Particle size distribution, concentration, and magnetic attraction affect transport of polymer-modified Fe0 nanoparticles in sand columns. *Environmental Science & Technology, 43* (13), 5079–5085.

Phenrat, T., Cihan, A., Kim, H. J., Mital, M., Illangasekare, T., & Lowry, G. V. (2010). Transport and deposition of polymer-modified Fe0 nanoparticles in 2-D heterogeneous porous media: Effects of particle concentration, Fe0 content, and coatings. *Environmental Science & Technology, 44* (23), 9086–9093.

Pitois, A., Abrahamsen, L. G., Ivanov, P. I., & Bryan, N. D. (2008). Humic acid sorption onto a quartz sand surface: A kinetic study and insight into fractionation. *Journal of Colloid and Interface Science, 325* (1), 93–100.

Rahman, M. A., Jose, S. C., Nowak, W., & Cirpka, O. A. (2005). Experiments on vertical transverse mixing in a large-scale heterogeneous model aquifer. *Journal of Contaminant Hydrology, 80* (3-4), 130–148.

Raychoudhury, T., Naja, G., & Ghoshal, S. (2010). Assessment of transport of two polyelectrolyte-stabilized zero-valent iron nanoparticles in porous media. *Journal of Contaminant Hydrology, 118* (3-4), 143–151.

Rebhun, M., De Smedt, F., & Rwetabula, J. (1996). Dissolved humic substances for remediation of sites contaminated by organic pollutants. Binding-desorption model predictions. *Water Research, 30* (9), 2027–2038.

Revil, A., Pezard, P. A., & Glover, P. W. (1999). Streaming potential in porous media: 1. Theory of the zeta potential. *Journal of Geophysical Research: Solid Earth (1978-2012), 104* (B9), 20021–20031.

Ryan, J. N., & Elimelech, M. (1996). Colloid mobilization and transport in groundwater. *Colloids and surfaces A: Physicochemical and engineering aspects, 107*, 1–56.

Saleh, N., Kim, H.-J., Phenrat, T., Matyjaszewski, K., Tilton, R. D., & Lowry, G. V. (2008). Ionic strength and composition affect the mobility of surface-modified Fe0 nanoparticles in water-saturated sand columns. *Environmental Science & Technology, 42* (9), 3349–3355.

Schmid, D., Micić Batka, V., Laumann, S., & Hofmann, T. (2015). Measuring the reactivity of commercial available zero-valent iron particles used for environmental remediation with iopromide. *Journal of Contaminant Hydrology, 181*, 36–45.

Sirk, K. M., Saleh, N. B., Phenrat, T., Kim, H.-J., Dufour, B., Ok, J., Golas, P. L., Matyaszewski, K., Lowry, G.V., & Tilton, R.D. (2009). Effect of adsorbed polyelectrolytes on nanoscale zero valent iron particle attachment to soil surface models. *Environmental Science & Technology, 43* (10), 3803–3808.

Stevenson, F. J. (1982). *Humus Chemistry: Genesis, Composition, Reactions*. New York: John Wiley & Sons.

Stieber, M., Putschew, A., & Jekel, M. (2008). Reductive dehalogenation of iopromide by zero-valent iron. *Water Science Technology, 57* (12), 1969–1975.

Tosco, T., & Sethi, R. (2010). Transport of non-newtonian suspensions of highly concentrated micro- and nanoscale iron particles in porous media: A modeling approach. *Environmental Science & Technology, 44* (23), 9062–9068.

Tosco, T., Gastone, F., & Sethi, R. (2014). Guar gum solutions for improved delivery of iron particles in porous media (Part 2): Iron transport tests and modeling in radial geometry. *Journal of Hydrology, 166*, 34–51.

Tratnyek, P. G., & Johnson, R. L. (2006). Nanotechnologies for environmental cleanup. *Nano today, 1* (2), 44–48.

Tucker, M. (2001). *Sedimentary petrology: An introduction to the origin of sedimentary rocks.* Malden, MA, USA: Blackwell Publishing.

Tufenkji, N., & Elimenech, M. (2004). Correlation equation for predicting single-collector efficiency in physicochemical filtration in saturated porous media. *Environmental Science & Technology, 38* (2), 529–536.

U.S. Environmental Protection Agency Office of Water (4303T). (2002). *Methods for measuring the acute toxicity of effluents and receiving waters to frehwater and marine organisms. Fifth edition. EPA-821-R-02-012*. Washington DC: U.S. Environmental Protection Agency Office of Water (4303T), 1200 Pennsylvania Avenue.

Verliefde, A., Cornelissen, E., Heijman, S., Petrinic, I., Luxbacher, T., Amy, G., Van der Bruggen, B., & van Dijk, J.C. (2009). Influence of membrane fouling by (pretreated) surface water on rejection of pharmaceutically active compounds (PhACs) by nanofiltration membranes. *Journal of Membrane Science, 330* (1-2), 90–103.

Vermöhlen, K., Lewandowski, H., Narres, H.-D., & Schwuger, M. (2000). Adsorption of polyelectrolytes onto oxides — the influence of ionic strength, molar mass, and Ca^{2+} ions, Colloids and Surfaces. *Physicochemical and Engineering Aspects, 163* (1), 45–53.

Wandruszka, R. v. (2000). Humic acids: Their detergent qualities and potential uses in pollution remediation. *Geochemical Transactions, 1* (1), 10–15.

Wankhede, S. B., Lad, K. A., & Chitlange, S. S. (2012). Development and validation of UV-spectrophotometric methods for simultaneous estimation of cetirizine hydrochloride and phenylephrine hydrochloride in tablets. *International journal of pharmaceutical sciences and drug research, 4* (3), 222–226.

Weishaar, J. L., Aiken, G. R., Bergamaschi, B. A., Fram, M. S., Fujii, R., & Mopper, K. (2003). Evaluation of Specific Ultraviolet Absorbance as an Indicator of the Chemical Composition and Reactivity of Dissolved Organic Carbon. *Environmental Science & Technology, 37* (20), 4702–4708.

Yang, D., Qiu, X., Zhou, M., & Lou, H. (2007). Properties of sodium lignin sulfonate as dispersant of coal water slurry. *Energy Conversation and Management, 48* (9), 2433–2438.

Yang, X., Flynn, R., Von der Kammer, F., & Hofmann, T. (2010). Quantifying the influence of humic acid adsorption on colloidal microsphere deposition onto iron-oxide-coated sand. *Environmental Pollution, 158* (12), 3498–3506.

Yao, K. M., Habibian, M. T., & O'Melia, C. R. (1971). Water and waste water filtration. Concepts and applications. *Environmental Science & Technology, 5* (11), 1105–1112.

Zhang, W. X. (2003). Nanoscale iron particles for environmental remediation: an overview. *Journal of nanoparticle Research, 5* (3-4), 323–332.

6.1 Internet links

[Image of lignin sulfonate monomer]. (3.4.2015). Retrieved from http://www.chemicalregister.com

Material safety data sheet according to regulation EC NO.: 1907/2006 [pdf]. (30.7.2015). Retrieved from www.nanoiron.cz/images/stories/msds_nanofer_25s.pdf

Bianco, C., Tosco, T., & Sethi, R. (20.7.2015). [MNMs 2015 v. 1007 software]. Retrieved from http://areeweb.polito.it/ricerca/groundwater/software/

7 Appendix

7.1 Appendix 1 – Properties of the natural sand

Table 3A - Recorded parameter during ζ potential measurements and long-term measurements of the sand in different aquifer modifier solutions				
Solution	ζ potential [mV]	pH	EC [mS m^{-1}]	T°C
MQ	-39.1	5.7	12.1	22.6
MQ 2 mg L^{-1} LS	-57.2	5.8	13.0	25.0
MQ 50 mg L^{-1} LS	-54.4	6.5	14.0	24.3
MQ 100 mg L^{-1} LS	-58.5	7.1	16.3	24.8
MQ 2 mg L^{-1} HU	-55.5	6.2	12.3	22.3
MQ 50 mg L^{-1} HU	-59.3	8.4	13.6	22.1
MQ 100 mg L^{-1} HU	-57.9	8.9	16.2	25.6
EPA	-25.0	8.0	28.6	23.4
EPA 50 mg L^{-1} LS	-27.2	8.2	31.6	24.4
EPA 100 mg L^{-1} LS	-25.3	8.1	32.3	23.5
EPA 50 mg L^{-1} HU	-24.5	8.2	30.8	24.3
EPA 100 mg L^{-1} HU	-22.2	8.4	30.7	23.7
Long-term experiments				
Solution	ζ potential [mV]	pH	EC [mS m^{-1}]	T°C
MQ 50 mg L^{-1} LS	-52.0	5.8	13.0	25.4
MQ 100 mg L^{-1} LS	-54.9	6.0	13.3	25.6
MQ 50 mg L^{-1} HU	-55.0	6.2	12.3	22.0
MQ 100 mg L^{-1} HU	-56.1	6.4	13.1	25.4
EPA 50 mg L^{-1} LS	-24.4	8.1	29.7	24.2
EPA 100 mg L^{-1} LS	-24.8	8.1	29.7	23.3
EPA 50 mg L^{-1} HU	-26.4	8.1	29.5	23.5
EPA 100 mg L^{-1} HU	-23.8	8.1	29.3	23.2

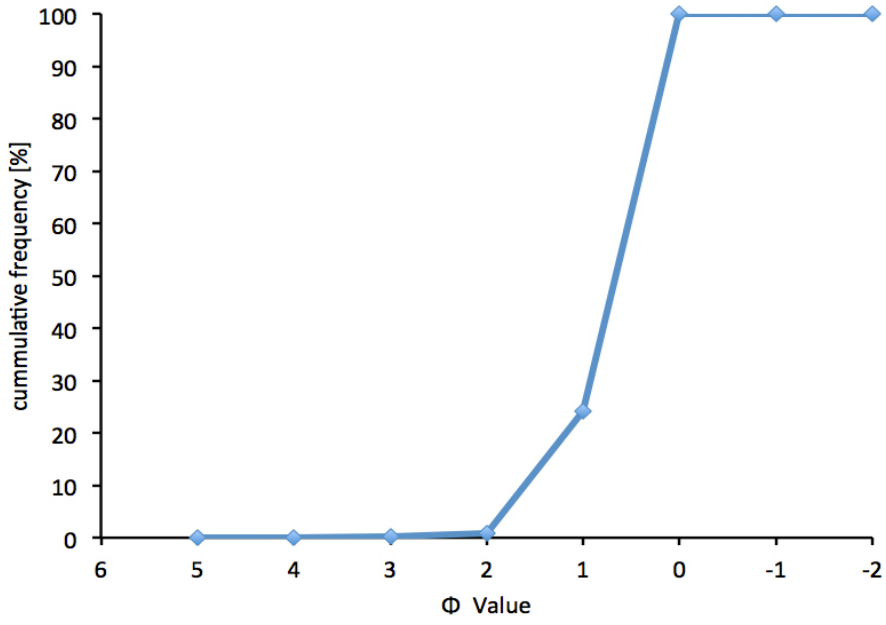

Fig. 9A – Sieving curve of Dorsilit Nr. 8 sand as a function of Φ Values according to Tucker et al. (2001)

Fig. 100A – Sampled suspension of white particle fraction flushed out oft the column. Observed after the flushing step in the long-term transport experiments

7.2 Appendix 2 – Calculated transport coefficients and MNMs model output data

Table 4A – Transport coefficients for nZVI calculated following Colloid Filtration Theory (Section 2.7)

Transport Experiments	Fe_{tot} C/C_0 [-]	$L_{T\,0.5}$ [m]	$L_{T\,0.37}$ [m]	$L_{T\,0.001}$ [m]	k_{CFT} [s^{-1}]	α [-]	η_0 [-]
MQ	0.33	0.06	0.09	0.63	0.012	0.40	0.019
MQ 50 mg L^{-1} LS	0.40	0.08	0.11	0.75	0.010	0.33	0.019
MQ 100 mg L^{-1} LS	0.50	0.10	0.14	0.99	0.008	0.25	0.019
MQ 50 mg L^{-1} HU	0.23	0.05	0.07	0.47	0.016	0.53	0.019
MQ 100 mg L^{-1} HU	0.25	0.05	0.07	0.49	0.016	0.50	0.019
EPA	0.03	0.02	0.03	0.20	0.038	0.27	0.088
EPA 50 mg L^{-1} LS	0.13	0.03	0.05	0.33	0.023	0.16	0.088
EPA 100 mg L^{-1} LS	0.10	0.03	0.04	0.30	0.025	0.18	0.088
EPA 50 mg L^{-1} HU	0.14	0.03	0.05	0.35	0.022	0.15	0.088
EPA 100 mg L^{-1} HU	0.16	0.04	0.05	0.37	0.021	0.14	0.088
Long-term transport experiments	Fe_{tot} C/C_0 [-]	$L_{T\,0.5}$ [m]	$L_{T\,0.37}$ [m]	$L_{T\,0.001}$ [m]	k_{CFT} [s^{-1}]	α [-]	η_0 [-]
MQ 50 mg L^{-1} LS	0.35	0.07	0.09	0.66	0.012	0.38	0.019
MQ 100 mg L^{-1} LS	0.47	0.09	0.13	0.93	0.008	0.27	0.019
MQ 50 mg L^{-1} HU	0.32	0.06	0.09	0.60	0.013	0.41	0.019
MQ 100 mg L^{-1} HU	0.59	0.13	0.19	1.30	0.006	0.19	0.019
EPA 50 mg L^{-1} LS	0.06	0.02	0.03	0.24	0.032	0.22	0.088
EPA 100 mg L^{-1} LS	0.07	0.03	0.04	0.26	0.030	0.21	0.088
EPA 50 mg L^{-1} HU	0.06	0.02	0.03	0.24	0.032	0.22	0.088
EPA 100 mg L^{-1} HU	0.10	0.03	0.04	0.29	0.026	0.18	0.088

Table 5A – Fitted MNMs model parameters for nZVI transport

Transport experiments	λ [-]	k_{a1} [s^{-1}]	k_{d1} [s^{-1}]	B [-]	A [-]	k_{a2} [s^{-1}]	k_{d2} [s^{-1}]
MQ	0.75	3.5E-05	1.6E-05	0.16	1000	0.079	0.12
MQ 50 mg L^{-1} LS	0.01	9.5E-03	6.0E-04	1.06	1000	1.243	1.00
MQ 100 mg L^{-1} LS	0.01	5.5E-03	1.3E-03	0.88	1000	1.618	1.00
MQ 50 mg L^{-1} HU	10.00	1.2E-02	3.6E-04	1.07	1000	1.000	0.71
MQ 100 mg L^{-1} HU	0.06	1.2E-02	1.1E-04	1.18	1000	1.606	1.00
EPA	2.10	3.2E-02	3.0E-05	1.36	1000	0.057	0.11
EPA 50 mg L^{-1} LS	10.00	2.0E-02	2.1E-04	1.17	1000	1.000	0.89
EPA 100 mg L^{-1} LS	10.00	1.7E-02	7.2E-04	1.19	1000	0.032	0.05
EPA 50 mg L^{-1} HU	4.23	4.2E-03	5.3E-04	0.72	1000	0.008	0.03
EPA 100 mg L^{-1} HU	9.32	1.0E-02	3.2E-04	0.97	1000	0.016	0.02
Long-term transport experiments	λ [-]	k_{a1} [s^{-1}]	k_{d1} [s^{-1}]	B [-]	A [-]	k_{a2} [s^{-1}]	k_{d2} [s^{-1}]
MQ 50 mg L^{-1} LS	0.76	1.3E-04	3.6E-04	0.32	1000	0.036	0.02
MQ 100 mg L^{-1} LS	0.61	9.3E-06	3.6E-05	0.01	1000	0.047	0.05
MQ 50 mg L^{-1} HU	0.10	9.6E-05	1.7E-04	0.28	1000	0.039	0.03
MQ 100 mg L^{-1} HU	1.00	7.4E-06	5.6E-05	0.01	1000	0.031	0.02
EPA 50 mg L^{-1} LS	2.10	3.5E-02	9.2E-04	1.12	1000	0.075	0.10
EPA 100 mg L^{-1} LS	2.57	2.3E-02	1.0E+03	1.34	1000	0.064	0.10
EPA 50 mg L^{-1} HU	2.57	3.1E-02	1.0E-06	1.70	1000	0.071	0.10
EPA 100 mg L^{-1} HU	2.57	2.4E-02	2.7E-04	1.29	1000	0.023	0.02

Table 6A – Fitted MNMs model parameters for aquifer modifier transport				
	MQ		**EPA**	
	100 mg L^{-1} LS	100 mg L^{-1} HU	100 mg L^{-1} LS	100 mg L^{-1} HU
D [m]	0.0021	0.0022	1.00E-05	9.18E-04
K_d [L kg^{-1}]	1.78E-04	1.86E-04	2.24E-04	2.15E-04

7.3 Statutory Declaration

STATUTORY DECLARATION

I declare that I have authored this thesis independently, that I have not used other than the declared sources / resources and that I have explicitly marked all material which has been quoted either literally or by content from the used sources.

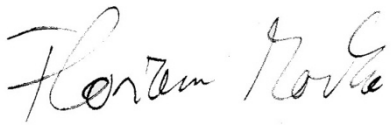

08.10.2015

…… ……..

Date (Signature)

7.4 Curriculum Vitae

Personal Information:

Name:	Florian Marko

Education:

Study

MSc Earth Sciences	(University of Vienna)	WS 12 – now
MSc Environmental Sciences	(University of Vienna)	WS 13 – now
BSc Earth Sciences	(University of Vienna)	WS 09 – WS 12
Theater, Film & Media Sciences	(University of Vienna)	WS 08 – SS 10
BSc Chemistry	(University of Vienna)	WS 08 – SS 10
BSc Earth Sciences	(K.F. University of Graz)	SS 08

Grammar School BRG Leibnitz	1999 – 2007
Elementary School St. Martin i.S.	1995 – 1999

Professional Experience:

• September 2013	Porr GmbH: Internship
• August 2013	Joaneum Research – RESOURCES: Internship
• August 2012	Geological Survey of Austria: Well mapping

Skills & Competences:

- Tutor at the TU Vienna 2012-2013
- Trained in REM, EPMA, EDX, UV-VIS, ICP-OES
- 8 months of Laboratory experience
- Digital image, video, music processing (Adobe Photoshop / Logic / Adobe Premiere); Microsoft Office
- Driving licence A and B

Additional Information

- Language stays in Phoenix, Arizona (Summer 2000 / Summer 2005)
- Participant at several extra-curricular geological excursions e.g. Bohemian Erzgebirge (July 2010), Kola Halfinsula (Aug. 2011), Cambodia/ Thailand (Feb.2012), Sri Lanka (Feb 2013)
- Travels to North, South America, Africa, Asia, Europe
- Founder and CEO of Chronic City Music Label; 10 years of professional music lessons (guitar), active as producer, songwriter and live-musician, multi instrumental performances in several bands and orchestras since the 14th year of age, more than 80 concerts played in Europe, several rotations in radio stations worldwide.
- 3. Price at the Styrian Mathematical Olympiad 2003, representative of BRG Leibnitz at the Austrian Mathematical Olympiad 2004

Languages:

German (Mother tongue), English (very good), Slovenian (A2)

Personal Interests:

Travelling, music, sport, literature, theater